Eur. Phys. J. B **56**, 35–39 (2007)
DOI: 10.1140/epjb/e2007-00087-5

THE EUROPEAN PHYSICAL JOURNAL B

Aligned single crystal Al-catalyzed boron nanorods on Si substrates

Qing Yang[1,2,a], Jian Sha[2], Lei Wang[2], Zhizhong Yuan[2], and Deren Yang[2,b]

[1] State Key Laboratory of Modern Optical Instrumentation, Zhejiang University, P.R. China
[2] State Key Lab of Silicon Materials, Zhejiang University, 310027 Hangzhou, P.R. China

Received 4 November 2005 / Received in final form 12 October 2006
Published online 28 March 2007 –

Abstract. Aligned tetragonal single crystal boron nanorods have been synthesized by chemical vapor deposition on silicon substrates without any templates. A thin film of Al was used as catalyst, and the nanorods were synthesized in a large area. The nanorods have a diameter of 20–50 nm. The SAED and HRTEM reveal that the nanorods are single crystal in nature and preferentially grew up along [002]. The optical properties of the nanorods were investigated. The growth mechanism of the boron nanorods has been discussed.

PACS. 81.07.Vb Quantum wires – 81.15.Gh Chemical vapor deposition (including plasma-enhanced CVD, MOCVD, etc.)

Introduction

Substantial effort has been placed on synthesizing semiconductor nanowires and nanotubes and developing them as building blocks for electronic devices. Silicon nanowires and carbon nanotubes have been studied most extensively [1–3]. The elemental boron, near to silicon and carbon in the periodic table, occupy a unique place within chemistry and physics for the complexity of the uncommon structures and many unique properties, such as high melting temperature, extreme hardness and lightness, unique transport and mechanical properties, etc. Recent theoretical studies [4–6] have suggested boron and carbon appeared to form a set of complementary chemical systems: whereas bulk carbon in its most stable form was characterized by a 2D system and carbon cluster were characterized by 3D cages; bulk boron was characterized by 3D cage, and boron cluster were characterized by 2D structures. It is interesting and important to synthesis boron nanostructures and to investigate their properties.

Recently, various one dimensional boron nanostructures have been fabricated, including amorphous [7–10] and crystalline boron nanowires (BNWs) [11–14], crystalline boron nanobelts [15], nanoribbons [16] and single wall boron nanotubes [17]. The synthesis methods are chemical vapor deposition (CVD) [10–12,16,17], laser ablation [15,18], vapor-transport method [9,14], and magnetron sputtering [7,8] etc. Among these methods, CVD is especially attractive because of the compatibility of CVD with conventional semiconductor device fabrication and also the ease of scaling research to production-size systems. And CVD method could allow controlled, selective growth of nanostructures by patterning metal catalysts on the substrates. So far Au and some other transition elements are the dominative catalysts for growing boron and other semiconductor nanowires in CVD synthesis system. Unfortunately, these metals trap electrons and holes in Si and pose a serious contamination problem for Si complementary metal oxide semiconductor (CMOS) processing. Especially for boron nanowire growth, the eutectic temperature of the transition metals and boron is generally high (>1000 °C), which requires high temperature during the growth. Main-group element aluminum is a standard metal in silicon process lines and might be an interesting alternative in order to incorporate nanowires in the front-end of a silicon IC. Additionally, the eutectic temperature of Al-B is 659.7 °C, much lower than the eutectic temperature of boron and other metals. From a technological standpoint, Al would be a much more attractive catalyst material for growth of boron nanowires. Previous study has confirmed that Al is an effective catalyst in growing high crystal aligned Si nanowires [19].

Aligned single crystalline BNWs [12] and MgB_2 nanowires [20] have been synthesized by our group by means of CVD and subsequent process using nanochannel-Al_2O_3 as the substrates. In this paper, we report the synthesis of aligned single crystal boron nanorods (BNRs) on silicon substrates using a thin film of Al as catalyst. The optical properties of the nanorods were also investigated.

Experiment

The experimental apparatus used in the work consists of a horizontal tube furnace (75 cm in length), a reacting

[a] e-mail: qingyang@zju.edu.cn
[b] e-mail: mseyang@ zju.edu.cn

chamber made of quartz tube ($\phi 5.5 \times 150$ cm), a rotary pump system, and a gas supply and control system. The ultimate vacuum for this configuration was ∼20 Pa. Several silicon (100) or (111) substrates were first cleaned in acetone by ultrasonic. Then, after cleaning the wafers by RCA and removing the native oxide with dilute HF, a thin film of Al with the thickness of about 5 nm was deposited on the silicon substrates by thermal evaporation system. The substrates were then placed in the center of the furnace for collecting the growth products. The reacting chamber was pumped down to 20 Pa and heated under Ar flow. As the temperature reached to the scheduled temperature in the range of 700–950 °C, the mixture gas of argon, hydrogen and diborane with a flow ratio of 50:20:1 was allowed into the chamber. The pressure in the chamber was kept at 5×10^4 Pa. After deposition for 5 h, the furnace was cooled down and the products were removed out and characterized by field emission scanning electron microscopy (FESEM, Siron, FEI). Then the nanorods were ultrasonically separated from the silicon substrates and characterized by transmission electron microscopy (TEM, CM200/Philips) equipped with energy dispersive X-ray spectrometer (EDX), selected area electron diffraction (SAED) and high resolution TEM (HRTEM). The optical absorbance measurements were performed with a Hitachi U-4100 UV-vis spectrophotometer. For comparison, the nanorods were also fabricated on the other substrates covered by a thin film Al such as silicon wafer with a thick dry oxide layer, quartz plates and nanochannel aluminum (NCA) in the same growth condition.

Results and discussion

FESEM images of the as-prepared BNRs on the silicon (100) substrates are shown in Figure 1. In order to know the most suitable growth conditions of the BNRs, the quartz tube were heated to a series of temperature ranged from 700 °C to 950 °C and kept for 5 h. Figure 1 shows the top-view FESEM images of the products synthesized at 700 °C, 800 °C, 900 °C, and 950 °C respectively. It was found that uniform large area BNR arrays can be fabricated in the temperature ranged from 800 °C to 900 °C. The density of the nanorods increased with the temperature increasing. The upper right inset in Figures 1b and 1c are the side view images of the aligned BNRs. It can be seen that the nanorods are aligned parallel with each other and perpendicular to the substrates. Porous boron films formed when the temperature was lower than 750 °C and higher than 950 °C. Uneven and very short BNRs could be observed when the temperature was in the range of 750–800 °C and 900–950 °C. The fluidness of catalyst alloy under different temperature might be the main reason for the difference morphology formed at different temperature. When the temperature was too low, aluminum films can't form alloy droplets which act as catalysts to lead the growth of nanorods. When the temperature was too high, aluminum films were not stable and could move easily, the alloy droplets were also unstable to lead the growth of the nanorods.

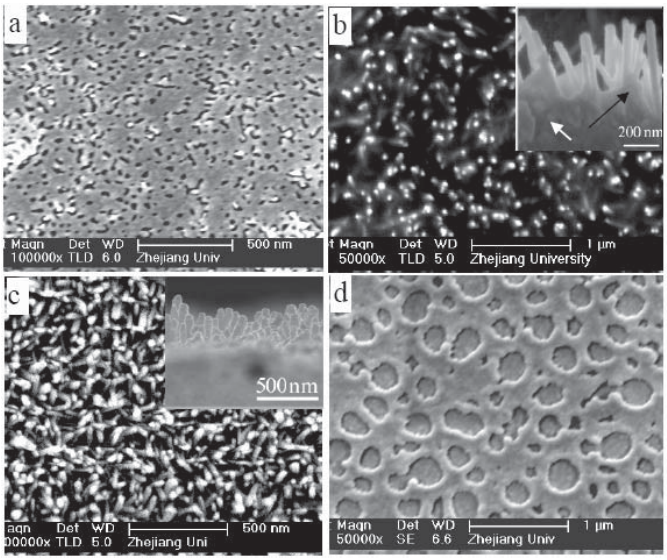

Fig. 1. FESEM images of the boron nanorods on the Si (100) substrates synthesized at different temperature, (a) 700 °C, (b) 800 °C, (c) 900 °C, and (d) 950 °C, the inset images shown in Figures 1b and 1c are the cross-sectional FESEM images of the boron nanorods at 800 °C and 900 °C, respectively.

The morphologies of BNRs on different substrates such as NCA, Si (111), Si substrates with oxide layer and quartz plates were also investigated. The FESEM images of them are shown in Figures 2a–2d respectively. The inset images in Figures 2a–2c are cross-sectional FESEM images of the BNRs on different substrates. As reported in the previous paper [12], the nanorods in NCA are aligned parallel with each other and the alignment of the nanorods on Si (100) substrates is as good as that in NCA (Figs. 1b, 1c and 2a). The alignment of the nanorods on Si (111) decreased slightly. However, the nanorods on Si substrates with thick oxide layer and quartz plates couldn't align in arrays and grew randomly.

The TEM image of the BNRs on Si (100) (Fig. 3) indicates that the nanorods have a diameter of 20–50 nm. The inset is SAED pattern of an individual nanorod, which illustrates the nanorod is single crystal tetragonal lattice structure of elemental boron with the lattice constant of $a = 8.73$ Å and $c = 5.06$ Å, the same structure as that reported in reference [12]. The nanorods in Figure 3 were also analyzed by EDX (Fig. 3b). Only carbon, copper and boron were detected. The carbon and copper originated from the copper grid covered with carbon film. Thus, the results of EDX also indicate that the fabricated nanorods are pure BNRs. The microstructure of a boron nanorod was characterized by HRTEM, as shown in Figures 3c and 3d. The HRTEM images show that the nanorod is single crystalline without the presence of dislocations, and its geometrical shape is uniform. There is a very thin amorphous oxide layer on the outside shell of the nanorod. An enlarged atomic image taken from Figure 3c is shown in Figure 3d. The distance between the parallel fringes is about 0.44 nm, corresponding to the spacing of (200) planes of B with P $\overline{4}$ n2 structure, which

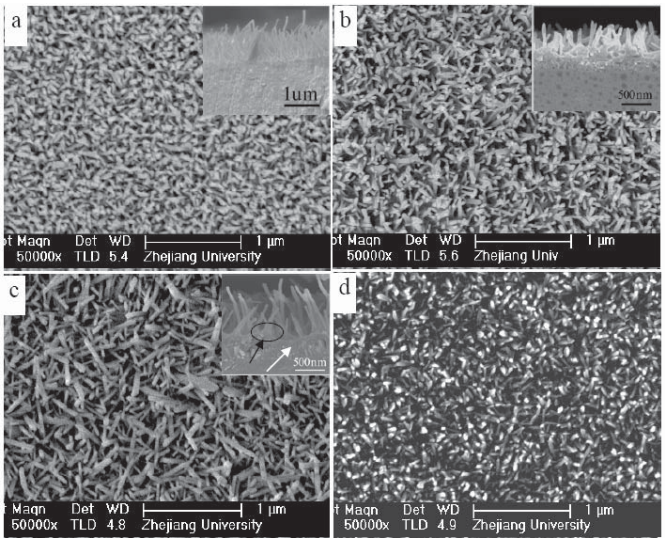

Fig. 2. FESEM images of the BNRs on different substrates, (a) NCA, (b) Si (111), (c) Si (111) with oxide layer, and (d) quartz plates, the inset images are cross-sectional view image of them.

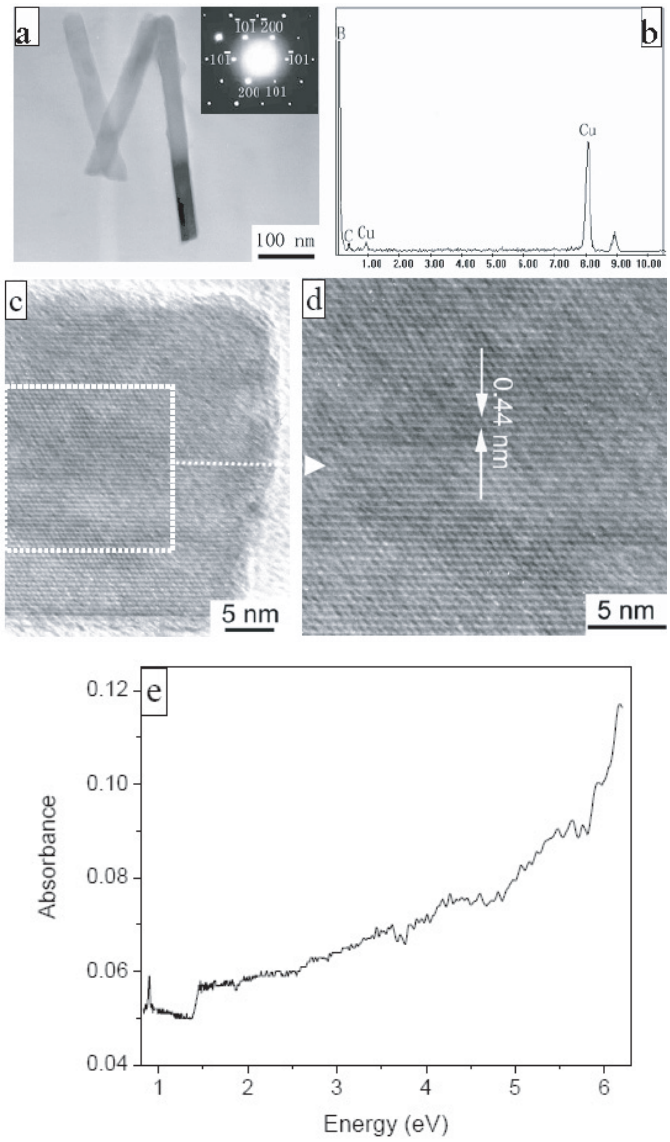

Fig. 3. TEM and optical characterization of the BNRs. (a) TEM image, the upper right inset image corresponds to the SAED pattern of a relative boron nanorod. (b) EDX spectrum of the boron nanorods. (c) HRTEM image, and (d) the enlarged atomic image of an individual boron nanorod revealing perfect single crystal structure. (e) Room-temperature optical absorbance spectra for BNRs.

is consistent with the SAED pattern. From the results of HRTEM, it can be indicated that the growth direction of the nanorods is [002]. An interesting thing is that alloy droplets can't be observed at the tips of the nanorods. Furthermore, a large number of nanorods were intensively investigated by TEM, all the nanorods had clean tips, and no metal droplet-terminated nanorods were identified. However, it was found that the aluminum catalyst was necessary for the growth of the nanorods in the experiment. The nanorods synthesized on other substrates were also investigated by TEM. Most of the nanorods have the same growth direction and similar morphology. The phenomena indicate that the growth mechanism of boron nanorods catalyzed by Al is complex which needed studying further.

There have been several theoretical calculations on the electronic structures and optical properties of boron crystals like α-rhombohedral B_{12} [21,22] and tetragonal crystals [21]; however, there is relatively little experimental measurement on the optical properties of boron crystals [23] especially tetragonal crystals. The optical properties of the tetragonal BNRs were investigated in the work. Figure 3e shows the UV-vis absorbance spectra for the nanorods on quartz plates. Since quartz is transparent in the 0.50–6.20 eV range, it is believed that the spectra are from BNRs. The calculation results showed that $\alpha{-}t{-}B_{50}$ was a metal with a semiconductor-like band structure near the Fermi level [21]. The curve here shows a strong peak at 0.90 eV, an absorption threshold at 1.37 eV, and the absorption steadily increases until 5.80 eV, and then the absorption increases very rapidly, reaching a main peak at 6.15 eV. Since the highest frequency of the spectrometer is 6.20 eV, the peaks beyond it can't be observed. The existence of absorption threshold at 1.37 eV indicates that the boron nanorods synthesized here are semiconductor, which is different with the calculation results [21], but agree with the electrical measurement results [24]. Further investigation including calculation is needed to understand optical properties of boron nanostructures.

Binary alloy phase diagram were used to understand the virtue of Al as catalyst and the growth mechanism of BNRs. It can be seen that the eutectic temperature of Al-B is 659.7 °C, lower than the eutectic temperature of Au-B (1056 °C), Fe-B (1174 °C) and Co-B (1110 °C), which might be helpful to grow the crystalline BNRs at low temperature. Since no catalyst droplets (the supporting of a conventional vapor-liquid-solid (VLS) growth mechanism) were present at the tips of the BNRs, a base-growth mechanism might be plausible. Aluminum silicide

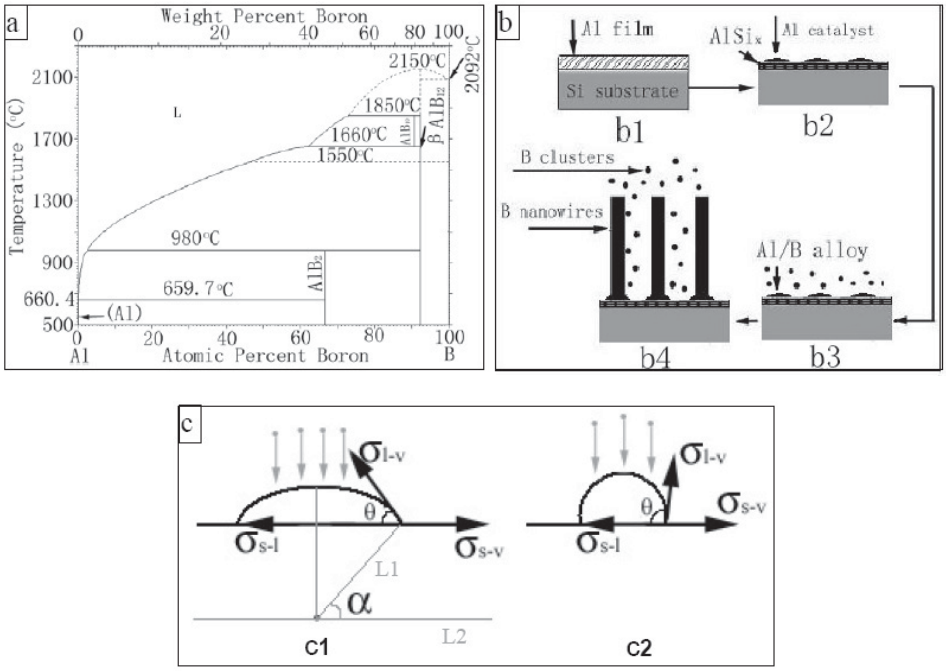

Fig. 4. Al-B phase diagram (a), growth schematic diagram of the aligned boron nanorods (b: b1-b4), and geometry of the catalyst droplets (c: c1, c2).

($AlSi_x$) was observed by cross-sectional FESEM at the silicon aluminum interface (Figs. 1b, 2c, marked by white arrows), which is the react products between aluminum and silicon. This reaction between the aluminum and silicon might increase the adhesion between the metal catalyst and the substrate, which could be one factor which caused the metal catalyst (Figs. 1b, 2c, marked by black arrows) staying at the base during the growth, and so the active growth surface is at the root of the nanorod, similar to the base growth of carbon nanotubes catalyst by Co [25]. The growth process of the BNRs might be as follows.

Firstly, when the temperature reached 800 °C, Al would melt and formed Al/Si interface and melting Al droplets (Fig. 4b2), since the eutectic temperature of Al-Si is 577 °C. The aluminum silicides consume a portion of the metallic aluminum and also serve as anchors or adhesion promoters for the melting Al droplets. Then boron atoms and/or clusters originated from the decomposition of diborane diffused into the liquid Al droplets to form Al/B liquid alloy (Fig. 4b3). Given the constant deposition temperature and a continuous precursor flux, the supersaturation Al/B liquid alloy could act as catalysts and directed the growth of BNRs (Fig. 4b4).

Circumstantiation about the reason why the catalysts stay at the bottom of the nanorods must combine the surface energy, atom diffusion and contact angle. At the NR/NW nucleation stage, there are two competitive processes, which is important for the selection of the NR/NW growth mode. One is the atom diffusion including surface and bulk diffusion from the top of the catalyst to the substrates. It is suggested that the mass transport rate of surface diffusion defined by the diffusion time τ_{di} is more important with decreasing whisker diameter [26]. So we just consider mass transport by the surface diffusion in the diffusion process. The other is the surface saturation and precipitation which can be defined by the saturation time τ_{sa}. It is easy understood that if $\tau_{di} > \tau_{sa}$, the catalyst droplet surface saturates with boron much faster than boron penetrates to the substrates, therefore, B precipitates at the droplet surface and the NR/NW growth mechanism is base growth. In contrast, if $\tau_{di} < \tau_{sa}$ B penetrates to the substrate faster than the catalyst droplet saturates, B precipitate at the bottom and the NR/NW growth mechanism is tip VLS growth, the catalyst droplet maintain on the tip of the NR/NW.

As shown in Figure 4c, if the adhesion between the substrate and catalyst is strong, contact angle θ is small (Fig. 4c1), contrarily, θ is large (Fig. 4c2). And the contact angle dominates the morphology of catalyst droplets. The angle α represents the angle between the line L1 (from any position on the catalyst to the center of the circle) and the line L2 (through the center of the circle parallel to the substrate surface). We can assume the boron atoms deposited vertically from the ambient atmosphere to the substrates. The boron atoms density distribution on the catalyst droplet can be expressed as:

$$C = C_0 \frac{\pi r^2[\cos^2\alpha - \cos^2(\alpha + d\alpha)]}{2\pi r * rd\alpha \cos\alpha} = KC_0 \sin\alpha.$$

Here C_0 represents the atoms density with a flat surface, K is a constant, and r is the radius of curvature of the droplet. According to Fick's first law, the material flux of surface diffusion J_S (quantity per unit time per unit length) represented by:

$$J_s = -D_s \frac{dC_s}{dl} = K' D_s C_0 \cos\alpha = K'' \cos\alpha.$$

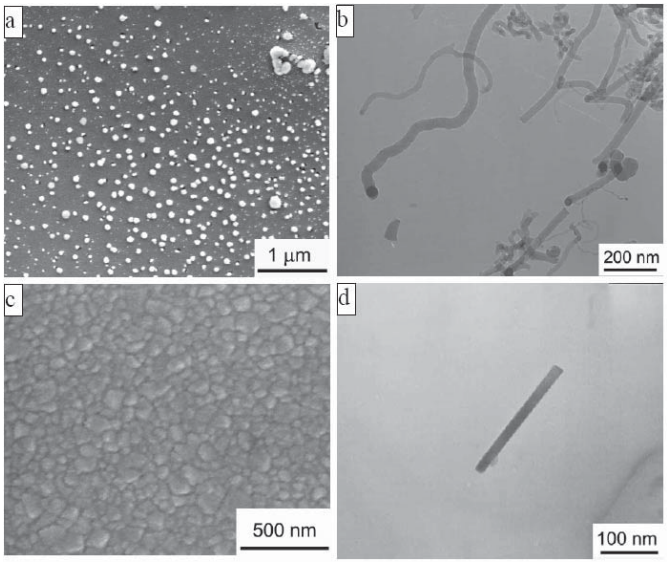

Fig. 5. FESEM images of the Au catalysts (a) and Al catalysts (c) annealed at 900 °C in vacuum for 20 min and removed for FESEM characterization. TEM images of the Au catalyzed boron nanowires (b), and Al catalyzed boron nanorods (d), boron nanowires and nanorods were synthesized by CVD at 900 °C seeded using the annealed Al and Au as catalysts.

It can be seen that α in Figure 4c1 is large and J_s is small or negative. In most area of the droplet in Figure 4c2, α is small and J_s is large. Therefore, if the droplet contact angle θ is small, the droplet surface easily saturates with boron and the NR/NW nucleate at the top of the droplet and the growth mechanism may be base growth. In contrast, if the droplet contact angle θ is large, the growth mechanism might be tip VLS growth. In order to validate the deduction, some other metals were used to growth BNR/BNW on silicon substrates. It is found that when the catalyst is Au and Ni, BNWs grew by tip VLS growth mechanism (Fig. 5b). Boron NR/NWs grew by base growth mechanism when the catalyst is Al and Ti (Fig. 5d). The morphology of the catalyst droplets were also investigated, we find that the contact angle of Au and Ni catalysts after high temperature annealing on silicon substrates is larger than that of Al and Ti (Figs. 5a, 5c): $\theta_{(\mathrm{Au,\ Ni})} > 90°$; $\theta_{(\mathrm{Al,\ Ti})} < 90°$. Further calculation and experiments are needed to understand the relation between the growth mechanism of NR/NWs and the catalyst droplet morphology.

Conclusions

In summary, single crystal BNRs have been synthesized by CVD on silicon substrates using a thin film of Al as catalyst without any templates. The nanorods were tetragonal phase and grew aligned in arrays. No metal nanoparticles were present at the tips of the nanorods. It is considered the growth mechanism of the nanorods is base-growth mechanism. The growth process and mechanism were deduced based on the analysis of the surface diffusion with different catalyst droplet morphology. The UV-vis spectrum shows a semiconductor band gap threshold at 1.37 eV and strong absorption at high frequency.

This work is financially supported by the National Natural Science Foundation of China (Project Nos. 50272057 and 60225010), and the key project of the Education Department of China.

References

1. Y. Wu, J. Xiang, C. Yang, W. Lu, C.M. Lieber, Nature **430**, 61 (2004)
2. C. Ye, L. Zhang, X. Fang, Y. Wang, P. Yan, J. Zhao, Adv. Mater. **16**, 1019 (2004)
3. A.I. Hochbaum, R. Fan, R. He, P. Yang, Nano Lett. **5**, 457 (2005)
4. I. Boustani, A. Quandt, E. Hernández, A. Rubio, J. Chem. Phys. **110**, 3176 (1999)
5. A. Gindulyte, W.N. Lipscomb, L. Massa, Inorg. Chem. **37**, 6544 (1998)
6. H.J. Zhai, B. Kiran, J. Li, L. Wang, Nature Mater. **2**, 827 (2003)
7. L.M. Cao, K. Hahn, Y. Wang, C. Scheu, Z. Zhang, C. Guo, Y. Li, X. Zhang, L. Sun, W. Wang, M. Rühle, Adv. Mater. **14**, 1294 (2002)
8. L.M. Cao, K. Hahn, C. Scheu, M. Rühle, Y.Q. Wang, Z. Zhang, C.X. Gao, Y.C. Li, X.Y. Zhang, M. He, L.L. Sun, W.K. Wang, Appl. Phys. Lett. **80**, 4226 (2002)
9. Y. Wu, B. Messer, P.D. Yang, Adv. Mater. **13**, 1487 (2001)
10. Q. Yang, J. Sha, L. Wang, Z. Su, X. Ma, J. Wang, D. Yang, J. Mater. Sci. **41**, 3547 (2006)
11. C.J. Otten, O.R. Lourie, M.F. Yu, J.M. Cowley, M.J. Dyer, R.S. Ruoff, W.E. Buhro, J. Am. Chem. Soc. **124**, 4564 (2002)
12. Q. Yang, J. Sha, J. Xu, Y. Ji, X. Ma, J. Niu, H. Hua, D. Yang, Chem. Phys. Lett. **379**, 87 (2003)
13. Y.Q. Wang, X.F. Duan, Appl. Phys. Lett. **82**, 272 (2003)
14. S.H. Yun, A. Dibos, J.Z. Wu, J.Z. Wu, Appl. Phys. Lett. **84**, 2892 (2004)
15. Z. Wang, Y. Shimizu, T. Sasaki, K. Kawaguchi, K. Kimura, N. Koshizaki, Chem. Phys. Lett. **368**, 663 (2003)
16. T.T. Xu, J. Zheng, N. Wu, A.W. Nicholls, J.R. Roth, D.A. Dikin, R.S. Ruoff, Nano Lett. **4**, 963 (2004)
17. D. Ciuparu, R.F. Klie, Y. Zhu, L. Pfefferle, J. Phys. Chem. B **108**, 3967 (2004)
18. X.M. Meng, J.Q. Hu, Y. Jiang, C.S. Lee, S.T. Lee, Chem. Phys. Lett. **370**, 825 (2003)
19. Y. Wang, V. Schmidt, S. Senz, U. Gosele, Nat. Nanotechno. **1**, 186 (2006)
20. Q. Yang, J. Sha, X. Ma, Y. Ji, D. Yang, Supercond. Sci. Technol. **17**, L31 (2004)
21. D. Li, Y. Xu, W.Y. Ching, Phys. Rev. B **45**, 5895 (1992)
22. S. Lee, D.M. Bylander, L. Kleinman, Phys. Rev. B **42**, 1316 (1990)
23. F.H. Horn, J. Appl. Phys. **30**, 1612 (1959)
24. K. Kawaguchi, K. Kirihara, Y. Shimizu, Z. Wang, Y. Shimizu, T. Sasaki, N. Koshizaki, K. Sogac, K. Kimura, Appl. Phys. Lett. **86**, 212101 (2005)
25. C. Bower, O. Zhou, W. Zhu, D.J. Werder, S. Jin, Appl. Phys. Lett. **77**, 2767 (2000)
26. H. Wang, G. Fischman, J. Appl. Phys. **76**, 1557 (1994)